

Progression of *PROM1*-Associated Retinal Degeneration as Determined by Spectral-Domain Optical Coherence Tomography Over a 24-Month Period



MANUEL GROSSPOETZL, REGINA RIEDL, GERNOT SCHLISSLEDER, ZHIHONG JEWEL HU, MICHEL MICHAELIDES, SRINIVAS SADDI, DAVID BIRCH, PETER CHARBEL ISSA, ANDREAS WEDRICH, GERALD SEIDEL, HENDRIK P.N. SCHOLL, AND RUPERT W. STRAUSS

- **PURPOSE:** To evaluate the progression of atrophy as determined by spectral-domain optical coherence tomography (SD-OCT) in patients with molecularly confirmed *PROM1*-associated retinal degeneration (RD) over a 24-month period.
- **DESIGN:** International, multicenter, prospective case series.
- **METHODS:** A total of 13 eyes (13 patients) affected with *PROM1*-associated RD were enrolled at 5 sites and SD-OCT images were obtained at baseline and after 24 months. Loss of mean thickness (MT) and intact area were estimated after semi-automated segmentation for the following individual retinal layers in the central subfield (CS), inner ring, and outer ring of the ETDRS grid: retinal pigment epithelium (RPE), outer segments (OS), inner segments (IS), outer nuclear layer (ONL), inner retina (IR), and total retina (TR).
- **RESULTS:** Statistically significant losses of thickness of RPE and TR were detected in the CS and inner ring and of ONL and IS in the outer ring (all $P < .05$); a statistically significant decrease in the intact area of RPE and IS was observed in the inner ring, and of ONL in the

outer ring (all $P < .05$); the change in MT and the intact area of the other layers showed a trend of decline over an observational period of 24 months.

- **CONCLUSIONS:** Significant thickness losses could be detected in outer retinal layers by SD-OCT over a 24-month period in patients with *PROM1*-associated retinal degeneration. Loss of thickness and/or intact area of such layers may serve as potential endpoints for clinical trials that aim to slow down the disease progression of *PROM1*-associated retinal degeneration. (Am J Ophthalmol 2024;259: 109–116. © 2023 The Authors. Published by Elsevier Inc. This is an open access article under the CC BY license (<http://creativecommons.org/licenses/by/4.0/>))

STARGARDT DISEASE TYPE 4 (STGD4) IS CAUSED BY disease-causing variants in the *PROM1* gene on chromosome 4.¹ These variants in *PROM1* can be inherited in an autosomal dominant (AD) trait as well as in an autosomal recessive (AR) trait.^{2,3} Whereas the AD form typically appears as a macular or Stargardt-like dystrophy, the AR form manifests as a cone-rod dystrophy or retinitis pigmentosa-like phenotype. Within the outer segments (OS) of the retina, the *PROM1* gene encodes the prominin 1 protein (*PROM1*; also known as CD133 and AC133), which is involved in the organization and formation of the photoreceptor disks.¹⁻³ Thus, a defective isoform of the *PROM1* protein is created that remains in the myoid region of the photoreceptors and cannot migrate to the OS site where the disks are formed, affecting the growth and organization of the photoreceptor disks.² Although there is not yet any currently approved therapy for STGD4,⁴ robust outcome measures such as disease progression or the changes of retinal layers over time are needed for future therapeutic approaches. To identify such potential endpoints and to gain a better understanding of the natural history of STGD4, a prospective longitudinal observational study was launched.⁵

Visual acuity is the most common clinical endpoint in ophthalmic research⁶; however, it has numerous limitations in inherited retinal dystrophies, including slow or delayed

AJO.com Supplemental Material available at AJO.com.

Hendrik P.N. Scholl and Rupert W. Strauss contributed equally and share senior authorship.

Accepted for publication November 10, 2023.

Department of Ophthalmology (M.G., G.S., A.W., G.S., R.W.S.), Medical University Graz, Graz, Austria; Institute for Medical Informatics, Statistics and Documentation (R.R.), Medical University Graz, Graz, Austria; Doheny Eye Institute (Z.J.H., S.V.S.), David Geffen School of Medicine at University of California Los Angeles, Los Angeles, California, USA; Moorfields Eye Hospital (M.M., R.W.S.), NHS Foundation Trust, London, United Kingdom; UCL Institute of Ophthalmology (M.M., R.W.S.), University College London, London, United Kingdom; Retina Foundation of the Southwest (D.B.), Dallas, Texas, USA; Department of Ophthalmology (P.C.I.), University of Bonn, Bonn, Germany; Oxford Eye Hospital (P.C.I.), Oxford University Hospitals NHS Foundation Trust, Oxford, United Kingdom; Nuffield Laboratory of Ophthalmology (P.C.I.), Department of Clinical Neurosciences, University of Oxford, Oxford, United Kingdom; Institute of Molecular and Clinical Ophthalmology Basel (H.P.N.S.), Basel, Switzerland; Department of Ophthalmology (R.W.S.), University of Basel, Basel, Switzerland; Wilmer Eye Institute (R.W.S.), Johns Hopkins University, Baltimore, Maryland, USA

Inquiries to Rupert W. Strauss, Medical University Graz, Graz, Austria; e-mail: r.strauss@medunigraz.at

© 2023 THE AUTHORS. PUBLISHED BY ELSEVIER INC.

THIS IS AN OPEN ACCESS ARTICLE UNDER THE CC BY LICENSE

([HTTP://CREATIVECOMMONS.ORG/LICENSES/BY/4.0/](http://creativecommons.org/licenses/by/4.0/))

progression, stable plateau phases, and a strong dependency on stable fixation and location of atrophic changes.⁶ In the analysis of progression of the ABCA4-related Stargardt disease cohort, it was found that visual acuity is not an appropriate main outcome measure for clinical trials, or else that it should be used only in distinct subgroups.⁷ Surrogate endpoints derived from retinal imaging are therefore needed, and have received support by the regulating authorities for treatments of macular diseases.⁸

Gene therapy using small molecule therapies such as anti-sense oligonucleotides, lentiviral vectors, adeno-associated viral vectors, or nanoparticles offer a strategy to selectively target specific stages of the visual cycle or elements of retinal function. Although these therapies may not offer a comprehensive cure, their primary aim is to alleviate symptoms and to impede the progression of the disease.⁹ Investigations have been conducted to explore the potential utility of molecular tools based on clustered regularly interspaced short palindrome repeats (CRISPR), with a particular focus on their application in the treatment of inherited retinal diseases.¹⁰⁻¹² It is conceivable that PROM1 may be responsive to one or more of the CRISPR-based methodologies currently documented, which encompass genome editing, epigenetic repression, base editing, and prime editing. Nevertheless, the identification of suitable candidates for these therapeutic interventions has posed a significant challenge, owing to the intricate role of PROM1 in the visual cycle. To date, there is no approved treatment option for PROM1-associated retinal degeneration.

Spectral-domain optical coherence tomography (SD-OCT) imaging allows visualization of the different retinal and choroidal layers and detection of morphological intraretinal changes that occur in macular diseases, and thus provides potential surrogate endpoints. Consequently, changes in SD-OCT have been selected as secondary endpoints in this study, with fundus autofluorescence being the primary endpoint in accordance to the ABCA4-related Prostar study.¹³ Herein, we present the estimated progression rates of atrophy derived from SD-OCT image analysis.

METHODS

• **PATIENTS AND PROCEDURES:** The study design, with inclusion and exclusion criteria as well as the study team at the participating sites, was previously described in detail.⁵ Briefly, patients (aged 6 years or older) with disease-causing variants in the PROM1 gene and well-demarcated atrophy in the primary study eye that did not exceed the 20° × 20° field of view in order to enable tracking by multimodal imaging including SD-OCT were eligible for enrollment. Clear ocular media and adequate pupillary dilation were required to ensure good quality of the image. The main exclusion criteria were other retinal diseases including choroidal

neovascularisation, diabetic maculopathy, epiretinal membrane, vascular diseases, and glaucoma.

• **SD-OCT AND GRADING MODALITIES:** At the participating sites, SD-OCT scans using a Heidelberg Spectralis device were obtained at baseline from a 20° × 20° scan area composed of 49 B-scans centered onto the anatomical fovea and, after 24 months, using the built-in follow-up mode. The Doheny Image Analysis Laboratory (DIAL) classification algorithm, an automated segmentation algorithm for SD-OCT scans, was applied to segment single retinal layers; algorithm errors were manually corrected using OCTOR 3.0 by 2 unmasked graders (M.G., G.S.) under consultation with a senior investigator (R.W.S.) in case of discrepancies. Images with insufficient quality (ungradable images) were excluded from analysis. SD-OCT scans were analysed with regard to changes in the mean thicknesses and intact areas of the retinal layers, which are described below, at baseline and after 24 months. Results were obtained for the central subfield (CS; 0.5-mm radius), the inner ring (IR; 0.5-1.5 mm), and the outer ring (OR 1.5-3 mm) of the Early Treatment of Diabetic Retinopathy Study (ETDRS) grid. Results were included only for retinal locations that could be imaged at both time points; that is, if patients developed a new preferred retinal locus during the observational period and consequently a different retinal region especially of the outer ring area was imaged, these regions were excluded from analysis. Right eyes as the primary study eyes were chosen for analysis, especially because PROM1-associated retinopathy is known to be a symmetrical disease of both eyes. We reviewed the 15 patients in our cohort for symmetry between right and left eyes, which could be observed in all patients. The detailed segmentation and analysis of individual layers has been described in detail previously¹⁴ and is provided in the Supplemental Material; in addition, it is illustrated in Figure 1. Of note, a minimum number of 25 B-scans were to be included per cube scan, per eye, and per visit, but the scans for inclusion were selected by the grader based on level of similarity to adjacent B-scans. Hence, if adjacent B-scans showed obvious qualitative differences in retinal sublayer thicknesses, they were both included, but if they were very similar, a gap of more than one B-scan between selected B-scans was permitted. However, all B-scans of the fovea center (and hence the central subfield of the ETDRS grid) had to be included.¹⁵

• **STATISTICAL METHODS:** Categorical data are presented as quantity and percentage, and continuous data are presented as mean and SD. To evaluate the change over time (from baseline to 24 months), linear models for repeated measures with endpoints (mean retinal thickness and intact area values) on the original scale, as well as square root-transformed endpoints (intact area values) as dependent variables and time as a continuous independent variable, were used. The β coefficients for time represent the yearly

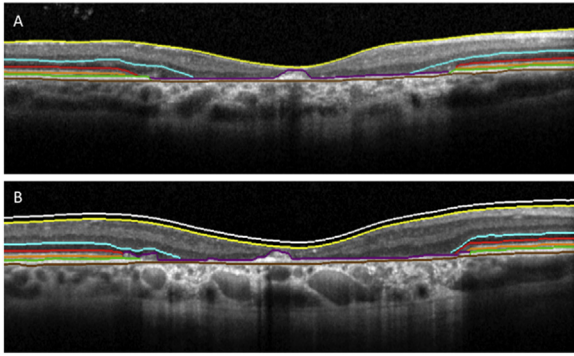


FIGURE 1. Segmentation of a patient's right eye diagnosed with PROM1-associated retinal degeneration; overlaid spectral-domain optical coherence tomography (SD-OCT) B-scans after manual segmentation at baseline and after 24 months. The segmented layers in order from top to bottom are as follows: vitreous top = white; internal limiting membrane = yellow; outer plexiform layer = blue; external limiting membrane = red; inner segments/outer segments = orange; photoreceptor segment layer = purple; retinal pigment epithelium = green; choroid = brown. A. SD-OCT B-scan of a patient's right eye showing an atrophic lesion of the outer retinal layers and central debris at baseline. B. The SD-OCT B-scan of the same eye after 24 months.

progression rates and are displayed with their corresponding standard errors (SEs).

P values <.05 were interpreted as statistically significant. SAS version 9.4 (SAS Inc.) was used for statistical analysis.

- **ETHICS CONSIDERATIONS:** The study was conducted according to the International Conference on Harmonisation of Technical Requirements for Registration of Pharmaceuticals for Human Use (ICH) Good Clinical Practice (GCP) Guidelines, the applicable regulatory requirements, and the current Declaration of Helsinki,¹⁶ and was in compliance with the Health Insurance Portability and Accountability Act if applicable. Ethics committee approval was granted by the local institutional review boards of the participating sites. The studies were registered at www.clinicaltrials.gov (identifier, NCT01977846). All patients gave informed consent before enrollment.

RESULTS

Images with insufficient quality (ungradable images) were excluded. In these patients, the images of the left eyes also showed insufficient quality for potential grading; hence, these patients were excluded. A total of 15 patients were enrolled in the study. Gradable images were available for 13 right eyes of 13 patients for both the baseline and the 24-month visit; information about disease-causing variants are provided in the Supplemental Table. Of these 13 patients, 6 were male and 7 female. The mean age (\pm SD) at baseline

was 38.2 ± 14.2 years, and mean age of onset of symptoms (available for 12 patients) was 30.3 ± 16.3 years. Mean best-corrected visual acuity (\pm SD) at baseline was 0.51 ± 0.53 logMAR. In all eyes, the same region of central subfield and inner ring could be imaged. In 6 of these eyes, the eye tracking option during follow-up could not be applied, and the cube scan covered different retinal locations with respect to the outer ring. Seven eyes with imaging of the same retinal regions were included in the analysis of the outer ring.

- **CENTRAL SUBFIELD:** At the baseline visit, 1 eye (7.7%) had a mean thickness of 0 for ONL, 7 eyes (53.8%) had mean thicknesses of 0 for IS, 9 eyes (69.2%) had mean thicknesses of 0 for OS, and 4 eyes (30.8%) had mean thicknesses of 0 for RPE. The RPE and the TR mean thickness showed statistically significant declines over 24 months. [Tables 1](#) and [2](#) show the mean retinal thicknesses and intact areas at the baseline and after 24 months in the central subfield. In estimation of progression rates, RPE and the TR mean thickness showed significantly declines over 24 months.

- **INNER RING OF ETDRS SUBFIELD:** The mean retinal thickness and intact area values in the inner ring of TR, IR, ONL, IS, OS, and RPE for the visits at baseline and after 24 months are summarized in [Tables 1](#) and [2](#). The mean RPE thickness, the intact area of the RPE, the mean TR thickness, and the intact area of the IS decreased significantly during the 24-month observation (all *P* < .05).

- **OUTER RING OF ETDRS SUBFIELD:** The ONL mean thickness, the ONL area, and the IS mean thickness showed statistically significant declines after 24 months ([Tables 1](#) and [2](#)). The ONL mean thickness declined with an estimated difference of -1.55 ± 0.481 μ m per year, the ONL area with an estimated decline of -0.062 ± 0.017 mm² per year, and the IS mean thickness with a thinning of -0.714 ± 0.238 μ m per year.

DISCUSSION

To the best of our knowledge, we present herein the first prospective cohort study with structural changes as determined by SD-OCT in PROM1-associated retinal degeneration. Statistically significant declines in mean thickness in RPE and TR thickness were identified within the central subfield CS and inner ring, as well as in ONL and IS thickness within the outer ring. Furthermore, a statistically significant decrease in the intact area of RPE and IS was observed in the inner ring, along with a reduction in the intact area of ONL in the outer ring. Moreover, during a 24-month observational period, there was an observed trend of declining macular thickness and intact area in other retinal layers.

TABLE 1. Estimated Annual Decline Rates in Central Subfield, Inner Ring, and Outer Ring of Progression of Mean Thicknesses of Examined Retinal Layers.

| Retinal Layers | Baseline Thickness (μm), Mean ± SD | | | Estimated Rate Difference in Progression (μm/y) of Mean Thickness, Coefficient ± SE | | | | | |
|----------------|------------------------------------|----------------|----------------|---|-------------|----------------|-------------|----------------|-------------|
| | Central subfield | Inner Ring | Outer Ring | Central Subfield | P Value | Inner Ring | P Value | Outer Ring | P Value |
| IR | 89.83 ± 16.61 | 141.29 ± 21.02 | 132.96 ± 12.70 | -1.981 ± 1.309 | .156 | -0.542 ± 0.062 | .399 | -0.029 ± 0.070 | .969 |
| ONL | 51.14 ± 30.53 | 42.44 ± 15.67 | 49.41 ± 16.62 | -1.112 ± 1.056 | .313 | -1.108 ± 0.651 | .114 | -1.550 ± 0.481 | .018 |
| IS | 10.35 ± 16.74 | 7.18 ± 10.82 | 19.71 ± 15.19 | -0.481 ± 0.405 | .259 | -0.600 ± 0.288 | .059 | -0.714 ± 0.238 | .024 |
| OS | 2.30 ± 4.19 | 1.38 ± 3.15 | 4.91 ± 4.63 | 0.069 ± 0.082 | .417 | -0.135 ± 0.093 | .172 | -0.307 ± 0.145 | .078 |
| RPE | 13.35 ± 12.73 | 14.35 ± 9.10 | 20.67 ± 4.60 | -1.935 ± 0.846 | .041 | -1.939 ± 0.511 | .003 | -1.321 ± 0.917 | .200 |
| TR | 183.75 ± 48.81 | 222.11 ± 34.77 | 232.60 ± 34.25 | -3.112 ± 0.965 | .007 | -2.746 ± 0.886 | .009 | -1.836 ± 0.904 | .089 |

IR = inner retina; IS = photoreceptor inner segment; ONL = outer nuclear layer; OS = photoreceptor outer segment; RPE = retinal pigment epithelium; TR = total retina.
 Boldface type denotes that progression is statistically significant ($P < .05$)

TABLE 2. Estimated Annual Growth Rates of Progression of Atrophy of Intact Area and Effective Lesion Radius, Determined From Square Root (Lesion Area /π) for Intact Area of Examined Retinal Layers.

| Retinal Layers | Baseline Value of Intact Area (mm ²), Mean ± SD | | | Estimated Rate Difference in Progression (mm ² /y) of Intact Area, Coefficient ± SE | | | | | | Estimated Rate Difference in Progression (mm/y) of Effective Lesion Radius Determined by Square Root, Coefficient ± SE | | | | | |
|----------------|---|-------------|--------------|--|---------|----------------|-------------|----------------|-------------|--|--------------|----------------|-------------|----------------|-------------|
| | Central Subfield | Inner Ring | Outer Ring | Central Subfield | P Value | Inner Ring | P Value | Outer Ring | P Value | Central Subfield | P Value | Inner Ring | P Value | Outer Ring | P Value |
| IR | 0.78 ± 0.00 | 6.28 ± 0.01 | 20.91 ± 0.41 | 0.001 ± 0.001 | 1.000 | 0.001 ± 0.001 | .585 | -0.019 ± 0.017 | .297 | 0.001 ± 0.001 | 1.000 | 0.001 ± 0.001 | .584 | -0.002 ± 0.002 | .296 |
| ONL | 0.72 ± 0.22 | 6.05 ± 0.74 | 20.87 ± 0.45 | 0.002 ± 0.003 | .387 | -0.050 ± 0.056 | .392 | -0.062 ± 0.017 | .011 | 0.001 ± 0.001 | .387 | -0.015 ± 0.017 | .373 | -0.007 ± 0.002 | .011 |
| IS | 0.25 ± 0.37 | 2.22 ± 2.47 | 14.93 ± 7.69 | 0.001 ± 0.002 | .673 | -0.114 ± 0.005 | .043 | -0.609 ± 0.276 | .070 | -0.003 ± 0.006 | .605 | -0.067 ± 0.027 | .031 | -0.123 ± 0.061 | .090 |
| OS | 0.20 ± 0.32 | 1.13 ± 1.77 | 11.96 ± 8.40 | -0.008 ± 0.009 | .346 | -0.194 ± 0.137 | .181 | -0.609 ± 0.293 | .083 | 0.004 ± 0.011 | .741 | -0.064 ± 0.087 | .283 | -0.067 ± 0.087 | .469 |
| RPE | 0.42 ± 0.38 | 4.44 ± 2.29 | 20.01 ± 2.23 | -0.033 ± 0.017 | .085 | -0.397 ± 0.132 | .011 | -0.413 ± 0.241 | .138 | -0.030 ± 0.013 | 0.040 | -0.128 ± 0.034 | .003 | -0.053 ± 0.034 | .168 |
| TR | 0.78 ± 0.01 | 6.28 ± 0.01 | 20.91 ± 0.41 | 0.001 ± 0.001 | 1.000 | 0.001 ± 0.001 | .585 | -0.019 ± 0.017 | .299 | 0.001 ± 0.001 | 1.000 | 0.001 ± 0.001 | .584 | -0.002 ± 0.002 | .296 |

IR = inner retina; IS = photoreceptor inner segment; ONL = outer nuclear layer; OS = photoreceptor outer segment; RPE = retinal pigment epithelium; TR = total retina.
 Boldface type denotes that progression is statistically significant ($P < .05$).

Imaging of the retina by SD-OCT has led to a better understanding of pathophysiology and changes in retinal degenerations leading to photoreceptor and RPE cell death, which can still be elusive. Both visualization of the photoreceptor band on SD-OCT as well as advantages of SD-OCT for assessing areas of atrophy, especially precision, safety, and patient comfort, were described previously. Furthermore, it might provide potential surrogate endpoints for future clinical trials.⁸

SD-OCT was chosen as a secondary endpoint in the *ABCA4*-associated STGD1 studies¹³ and, consecutively, also in the *PROM1*-associated STGD4 study, with fundus autofluorescence being the primary endpoint. It has been reported that the integrity of the EZ in patients with STGD1 correlates with differences in visual acuity, microperimetry sensitivity, and the extent of fundus lesions, as well as with multifocal ERG results; thus, the assessment of the EZ might be a particularly important parameter in STGD1.^{17–19} In another study, visual acuity was directly correlated with EZ/OS volume and inversely correlated with *en face* EZ loss/atrophy and attenuation of the OS/EZ.²⁰ However, there are significant differences between these STGD1 and STGD4, despite the common nomenclature. It was observed that in patients affected by STGD4, the disease may remain confined to the macular region. In the early phase of the disease, there is an increased foveal reflex and a red-speckled macular appearance that progresses to bull's-eye maculopathy (BEM), leading to macular atrophy over time.²¹ However, the exact pathogenesis is still poorly understood. The classic appearance with ring-shaped RPE atrophy and intact foveal center is possibly due to an increasing lipofuscin accumulation in the RPE, which is highest at the posterior pole and shows a depression at the fovea.^{22,23} With disease progression, the foveal center also becomes involved.²¹ It has been shown that *PROM1* is required for the maintenance of the expression levels of *ABCA4* and *RDH12*, which is consistent with the idea that *PROM1* is also involved in the regulation of the visual cycle, especially at the reducing step of all-trans-retinal to all-trans-retinol.⁴ Alternatively, *PROM1* may play an indirect role in lipofuscin accumulation through *ABCA4* dysfunction, resulting from a disrupted outer segment structure.^{24,25} These changes are also reflected in the results in our study, which showed that the RPE of the inner ring and the central subfield were particularly affected by atrophy. Two SD-OCT-derived variables in particular may serve as potential surrogate endpoints: a decrease in mean retinal thickness, and a decrease in the intact area (ie, thickness >0 μm at baseline). Although a decrease in mean retinal thickness may show only small differences over time (also, depending on grading protocols),²⁶ a decrease in an intact area can provide more robust parameters. However, a decrease in an intact area may depend on initial lesion size. To account for the initial size of the intact area of the retinal layers analyzed, we considered the radius determined by the square root of the area to better represent

the increase in atrophy, after significant differences were observed in our patient population regarding the initial size of the intact area. Use of square root transformation of lesion area measurements in patients with geographic atrophy has already been described in age-related macular degeneration, to eliminate the dependence of growth rates on original lesion size.²⁷ The square root strategy can simplify the design and enrollment in clinical trials because it may not be necessary to specify a range of lesion sizes or to include lesion size in the analysis.²⁷

It is known that, over the course of inherited macular and retinal dystrophies, there is a slow progressive loss of retinal function and structure, which, however, varies greatly among patients and individual families; this phenomenon has been reported not only in families and/or patients with *PROM1*-associated retinal dystrophies, but also other macular/panretinal degenerations.^{21,28–30} We could observe a decline in all retinal layers, although these were statistically significant only in distinct subretinal layers and distinct retinal locations over a time period of 2 years. It is known that *PROM1*-associated retinal degeneration shows only slow progression, and we did not know the onset age of the disease in the patients in our study. Therefore, a 24-month observation period might represent an insufficient time period. However, to the best of our knowledge, this study is the first to observe retinal thicknesses and intact retinal areas over a 24-month period in patients with *PROM1*-associated STGD4.

The investigation and classification of atrophy in STGD4 based on SD-OCT has proved to be difficult; the software algorithm applied led to many errors due to the hyperreflective debris in areas of atrophy frequently occurring in STGD4 (eg, in comparison to dry age-related macular degeneration), and therefore significant manual corrections were necessary.³¹ Indeed, similar observations were made in a preliminary study regarding *ABCA4*-related STGD1, and in up to 20.2% of B-scans, the outer retina was misidentified, and more than 30% of B-scans revealed significant software errors.³² Another preliminary analysis of repeatability of SD-OCT grading showed considerable noise in analysis of the RPE, with large variability in the difference between gradings (as indicated by poor intraclass correlations and also by the high relative absolute differences between gradings for thickness and intact area, whereas in measurements of thickness and intact area the inner and outer segments in the inner and outer ring regions had good to excellent intraclass correlations.²⁶ In addition, the phenotypes in the study presented herein showed a very heterogeneous appearance of *PROM1*-related STGD4, depending on the respective stage, and this proved to be a further challenge in the use, investigation, and quantification of the SD-OCT images.

These considerations must be kept in mind when analyzing the progression data. Because of the significant noise involved, it is important to consider that the progression of thicknesses and the measurement of intact areas may be ap-

appropriate only for certain subtypes of atrophy. The IS and OS (including the EZ), however, might serve as potential outcome measures.

Longitudinal data are dependent on the same location of the measurements. Although the imaging protocol required the photographers to center the 20° × 20° cube scan onto the anatomical fovea and then use the follow-up and eye-tracking function of the Heidelberg Spectralis device, patients often had an eccentric fixation due to pre-existing or developing atrophy, and the cube scan eventually could not be completely centered onto the anatomical fovea, or it led to a newly developing, preferred retinal locus. As a consequence, either already at baseline and/or during follow-up, some parts of the outer EDTRS ring were missing,³³ which we had to exclude for the purpose of this analysis.

Despite its multicenter design, our study has some limitations, especially the small number of cases (based on the fact that the number of reported patients affected by *PROM1*-associated retinal degenerations was even smaller at the time that the study was designed), and the fact that we could not include the stage of the disease of the individual patients. We were able to address this at least partially with respect to the size of the atrophic lesions and intact area by using the square root calculation; however, it may have had an impact on the mean thickness of the individual retinal layers examined.

Nevertheless, SD-OCT offers several advantages to provide possible surrogate outcome measures for upcoming clinical trials. With this examination modality, noninvasive, rapid examinations (in contrast to microperimetry, for example) can be performed, which can be standardized at different locations and which have no or only a low risk of potential retinal light toxicity (in contrast to fundus autofluorescence (FAF)).³⁴ Furthermore, it ensures the possibility of displaying the photoreceptors, or parts of them, and can therefore be accepted by regulatory authorities as a surrogate endpoint.⁸

SD-OCT seems to be a suitable examination tool especially in the early stages of the disease, when the patients still have a stable fixation, the central macula is predominantly affected, and changes occur especially in the area of the IS/OS (or EZ) rather than the RPE. Indeed, the group at 1 of the participating sites performed a deep phenotyping in 4 of the patients in this study and could show that FAF could have strong limitations in the early stages of the disease, whereas SD-OCT is a suitable tool to track progression.¹⁴ However, patients in early disease stages are the best candidates for pharmaceutical or gene therapy to rescue the remaining photoreceptors and/or RPE cells, or to protect them from impending degeneration.³⁵ Further studies are needed to correlate the structural changes with visual function parameters, such as those derived from photopic and/or scotopic microperimetry.^{28,36}

Funding/Support: Financial Disclosures: D.G.B.: grant support from AGTC/Beacon, 4D MT, PYC Therapeutics, Ocugen; Scientific Advisory Board for Nacuity Pharma, FFB; consults for Editas, 4D MT, PYC Therapeutics, ONL Therapeutics, Bluerock Therapeutics, Aldyra. P.C.I.: National Institute for Health Research (NIHR) Oxford Biomedical Research Centre (BRC); H.S.: support from the [Swiss National Science Foundation](#) (Project funding: “Developing novel outcomes for clinical trials in Stargardt disease using structure/function relationship and deep learning” #310030_201165, and National Center of Competence in Research Molecular Systems Engineering: “NCCR MSE: Molecular Systems Engineering (phase II)” #51NF40-182895), the Wellcome Trust (PINNACLE study), and the Foundation Fighting Blindness Clinical Research Institute (ProgStar study). H.S. is co-director of the Institute of Molecular and Clinical Ophthalmology Basel (IOB), which is constituted as a non-profit foundation and receives funding from the University of Basel, the University Hospital Basel, Novartis, and the government of Basel-Stadt. M.M.: award from the National Institute for Health Research Biomedical Research Centre at Moorfields Eye Hospital NHS Foundation Trust and UCL Institute of Ophthalmology, London, United Kingdom. member of the Scientific Advisory Board of: Ascidian Therapeutics, Inc.; Boehringer Ingelheim Pharma GmbH & Co; Droia NV; Eluminex Biosciences; Gyroscope Therapeutics Ltd.; Janssen Research & Development, LLC (Johnson & Johnson); Okuvision GmbH; ReVision Therapeutics Inc.; and Saliogen Therapeutics Inc. H.S. is a consultant of: Alnylam Pharmaceuticals Inc.; Gerson Lehrman Group Inc.; Guidepoint Global, LLC; and Tenpoint Therapeutics. H.S. is member of the Data Monitoring and Safety Board/Committee of Belite Bio (DRAGON trial, NCT05244304; LBS-008-CT02, NCT05266014), F. Hoffmann-La Roche Ltd (VELODROME trial, NCT04657289; DIAGRID trial, NCT05126966; HUTONG trial), ViGeneron (“A Prospective, Open-label, Phase 1b, Single-arm, Safety Study of an Intravitreal Application of a Recombinant Adeno-associated Virus Vector Expressing CNGA1 (AAV2.NN-CNGA1) in Patients with Retinitis Pigmentosa Due to CNGA1 Mutations” study, ViGeneron’s protocol number VG901-2021-A) and member of the Steering Committee of Novo Nordisk (FOCUS trial; NCT03811561). R.S.: support from the Foundation Fighting Blindness Clinical Research Institute (FFBCRI). S.V.S.: consulting fees from Apellis, Amgen, Abbvie/Allergan, Samsung Bioepis, Biogen, Boehringer Ingelheim, Iveric, Notal, Novartis, Roche, Bayer, Regeneron, Pfizer, Astellas, Nanoscope, Janssen, Centervue, Oxurion, Optos, and Heidelberg, and honoraria for lectures from Novartis, Roche, Optos, and Heidelberg. S.V.S. is a member of the Data Safety Monitoring/Advisory Board of Regeneron and holds leadership/fiduciary roles in ARVO and Macula Society. All arrangements have been reviewed and approved by the University of Basel (Universitätsspital Basel [USB]) and the Board of Directors of the Institute of Molecular and Clinical Ophthalmology Basel (IOB) in accordance with their conflict of interest policies. Compensation is being negotiated and administered as grants by USB which receives them on its proper accounts. All other authors report no financial disclosures or conflicts of interest. All authors attest that they meet the current ICMJE criteria for authorship. Acknowledgment: The Department of Ophthalmology Medical University Graz is an affiliated member of the European Network for Orphan Diseases (ERN-EYE).

REFERENCES

1. Kniazeva M, Chiang MF, Morgan B, et al. A new locus for autosomal dominant Stargardt-like disease maps to chromosome 4. *Am J Hum Genet.* 1999;64(5):1394–1399. doi:10.1086/302377.
2. Yang Z, Chen Y, Lillo C, et al. Mutant prominin 1 found in patients with macular degeneration disrupts photoreceptor disk morphogenesis in mice. *J Clin Invest.* 2008;118(8):2908–2916. doi:10.1172/JCI35891.
3. Maw MA, Corbeil D, Koch J, et al. A frameshift mutation in

- prominin (mouse)-like 1 causes human retinal degeneration. *Hum Mol Genet.* 2000;9(1):27–34. doi:10.1093/hmg/9.1.27.
4. Dellett M, Sasai N, Nishide K, et al. Genetic background and light-dependent progression of photoreceptor cell degeneration in prominin-1 knockout mice. *Invest Ophthalmol Vis Sci.* 2015;56(1):164–176. doi:10.1167/iovs.14-15479.
 5. Strauss RW, Muñoz B, Ahmed MI, et al. The progression of the Stargardt Disease Type 4 (ProgStar-4) Study: design and baseline characteristics (ProgStar-4 Report No. 1). *Ophthalmic Res.* 2018;60(3):185–194. doi:10.1159/000491791.
 6. Beck RW, Maguire MG, Bressler NM, Glassman AR, Lindblad AS, Ferris FL. Visual acuity as an outcome measure in clinical trials of retinal diseases. *Ophthalmology.* 2007;114(10):1804–1809. doi:10.1016/j.ophtha.2007.06.047.
 7. Kong X, Fujinami K, Strauss RW, et al. Visual acuity change over 24 months and its association with foveal phenotype and genotype in individuals with Stargardt disease. *JAMA Ophthalmol.* 2018;136(8):920–928. doi:10.1001/jamaophthalmol.2018.2198.
 8. Csaky K, Ferris F, Chew EY, Nair P, Cheetham JK, Duncan JL. Report from the NEI/FDA Endpoints Workshop on Age-Related Macular Degeneration and Inherited Retinal Diseases. *Invest Ophthalmol Vis Sci.* 2017;58(9):3456. doi:10.1167/iovs.17-22339.
 9. Piotter E, McClements ME, MacLaren RE. Therapy approaches for Stargardt disease. *Biomolecules.* 2021;11(8):1179. doi:10.3390/biom11081179.
 10. Kantor A, McClements ME, Peddle CF, et al. CRISPR genome engineering for retinal diseases. *Progress in Molecular Biology and Translational Science* Elsevier; 2021:29–79. doi:10.1016/bs.pmbts.2021.01.024.
 11. Peddle CF, Fry LE, McClements ME, MacLaren RE. CRISPR interference—potential application in retinal disease. *Int J Mol Sci.* 2020;21(7):2329. doi:10.3390/ijms21072329.
 12. Quinn J, Musa A, Kantor A, et al. Genome-editing strategies for treating human retinal degenerations. *Hum Gene Ther.* 2021;32(5-6):247–259. doi:10.1089/hum.2020.231.
 13. Strauss RW, Ho A, Muñoz B, et al. The Natural History of the Progression of Atrophy Secondary to Stargardt Disease (ProgStar) Studies. *Ophthalmology.* 2016;123(4):817–828. doi:10.1016/j.ophtha.2015.12.009.
 14. Schließleder G, Kalitzeos A, Kasilian M, et al. Deep phenotyping of PROM1-associated retinal degeneration. *Br J Ophthalmol.* 2023 Published online April 20;bjoo-2022-322036. doi:10.1136/bjo-2022-322036.
 15. Velaga SB, Nittala MG, Jenkins D, et al. Impact of segmentation density on spectral domain optical coherence tomography assessment in Stargardt disease. *Graefes Arch Clin Exp Ophthalmol.* 2019;257(3):549–556. doi:10.1007/s00417-018-04229-3.
 16. World Medical Association World Medical Association Declaration of Helsinki: ethical principles for medical research involving human subjects. *JAMA.* 2013;310(20):2191. doi:10.1001/jama.2013.281053.
 17. Birch DG, Locke KG, Felius J, et al. Rates of decline in regions of the visual field defined by frequency-domain optical coherence tomography in patients with RPGR-mediated X-linked retinitis pigmentosa. *Ophthalmology.* 2015;122(4):833–839. doi:10.1016/j.ophtha.2014.11.005.
 18. Testa F, Melillo P, Di Iorio V, et al. Macular function and morphologic features in juvenile Stargardt disease. *Ophthalmology.* 2014;121(12):2399–2405. doi:10.1016/j.ophtha.2014.06.032.
 19. Testa F, Rossi S, Sodi A, et al. Correlation between photoreceptor layer integrity and visual function in patients with Stargardt disease: implications for gene therapy. *Invest Ophthalmol Vis Sci.* 2012;53(8):4409. doi:10.1167/iovs.11-8201.
 20. Arepalli S, Traboulsi EI, Ehlers JP. Ellipsoid zone mapping and outer retinal assessment in Stargardt disease. *Retina.* 2018;38(7):1427–1431. doi:10.1097/IAE.0000000000001716.
 21. Michaelides M, Gaillard MC, Escher P, et al. The PROM1 mutation p.R373C causes an autosomal dominant bull's eye maculopathy associated with rod, rod-cone, and macular dystrophy. *Invest Ophthalmol Vis Sci.* 2010;51(9):4771. doi:10.1167/iovs.09-4561.
 22. von Rückmann A, Fitzke FW, Bird AC. Fundus autofluorescence in age-related macular disease imaged with a laser scanning ophthalmoscope. *Invest Ophthalmol Vis Sci.* 1997;38(2):478–486.
 23. Wing GL, Blanchard GC, Weiter JJ. The topography and age relationship of lipofuscin concentration in the retinal pigment epithelium. *Invest Ophthalmol Vis Sci.* 1978;17(7):601–607.
 24. Gliem M, Müller PL, Birtel J, et al. Quantitative fundus autofluorescence and genetic associations in macular, cone, and cone-rod dystrophies. *Ophthalmol Retina.* 2020;4(7):737–749. doi:10.1016/j.oret.2020.02.009.
 25. Mishra Z, Wang Z, Sada SR, Hu Z. Automatic segmentation in multiple OCT layers For Stargardt disease characterization via deep learning. *Transl Vis Sci Technol.* 2021;10(4):24. doi:10.1167/tvst.10.4.24.
 26. Kong X, Ho A, Munoz B, et al. Reproducibility of measurements of retinal structural parameters using optical coherence tomography in Stargardt disease. *Transl Vis Sci Technol.* 2019;8(3):46. doi:10.1167/tvst.8.3.46.
 27. Feuer WJ, Yehoshua Z, Gregori G, et al. Square root transformation of geographic atrophy area measurements to eliminate dependence of growth rates on baseline lesion measurements: a reanalysis of age-related eye disease study report no. 26. *JAMA Ophthalmol.* 2013;131(1):110. doi:10.1001/jamaophthalmol.2013.572.
 28. Tanna P, Georgiou M, Aboshiha J, et al. Cross-sectional and longitudinal assessment of retinal sensitivity in patients with childhood-onset Stargardt disease. *Transl Vis Sci Technol.* 2018;7(6):10. doi:10.1167/tvst.7.6.10.
 29. Palejwala NV, Gale MJ, Clark RF, Schlechter C, Weleber RG, Pennesi ME. Insights into autosomal dominant Stargardt-like macular dystrophy through multimodality diagnostic imaging. *Retina.* 2016;36(1):119–130. doi:10.1097/IAE.0000000000000659.
 30. Zhang Q, Zulfiqar F, Xiao X, et al. Severe retinitis pigmentosa mapped to 4p15 and associated with a novel mutation in the PROM1 gene. *Hum Genet.* 2007;122(3-4):293–299. doi:10.1007/s00439-007-0395-2.
 31. Garrity ST, Sarraf D, Freund KB, Sada SR. Multimodal imaging of nonneovascular age-related macular degeneration. *Invest Ophthalmol Vis Sci.* 2018;59(4):AMD48. doi:10.1167/iovs.18-24158.

32. Strauss RW, Muñoz B, Wolfson Y, et al. Assessment of estimated retinal atrophy progression in Stargardt macular dystrophy using spectral-domain optical coherence tomography. *Br J Ophthalmol*. 2016;100(7):956–962. doi:[10.1136/bjophthalmol-2015-307035](https://doi.org/10.1136/bjophthalmol-2015-307035).
33. Schönbach EM, Strauss RW, Kong X, et al. Longitudinal changes of fixation location and stability within 12 months in Stargardt disease: ProgStar report no. 12. *Am J Ophthalmol*. 2018;193:54–61. doi:[10.1016/j.ajo.2018.06.003](https://doi.org/10.1016/j.ajo.2018.06.003).
34. Strauss R, Muñoz B, Jha A, et al. Comparison of short-wavelength reduced-illuminance and conventional autofluorescence imaging in Stargardt macular dystrophy. *Am J Ophthalmol*. 2016;168. doi:[10.1016/j.ajo.2016.06.003](https://doi.org/10.1016/j.ajo.2016.06.003).
35. Scholl HPN, Strauss RW, Singh MS, et al. Emerging therapies for inherited retinal degeneration. *Sci Transl Med*. 2016;8(368). doi:[10.1126/scitranslmed.aaf2838](https://doi.org/10.1126/scitranslmed.aaf2838).
36. Strauss RW, Kong X, Bittencourt MG, et al. Scotopic Microperimetric Assessment of Rod Function in Stargardt Disease (SMART) Study: design and baseline characteristics (report no. 1). *Ophthalmic Res*. 2019;61(1):36–43. doi:[10.1159/000488711](https://doi.org/10.1159/000488711).